International Journal of Advances in Applied Sciences (IJAAS)
Vol. 13, No. 4, December 2024, pp. 777~786
ISSN: 2252-8814, DOI: 10.11591/ijaas.v13.i4.pp777-786

Potentiometric field-effect transistor pH sensing in a low-power wide-area network

Akmal Mustaffa Zulhakim[1], Wan Fazlida Hanim Abdullah[1], Ahmad Zaki Abu Bakar[2], Robaiah Mamat[1], Ili Shairah Abdul Halim[1], Muhammad Izzat Alif Muslan[1], Sukreen Hana Herman[1]
[1]Integrated Sensors Research Group, School of Electrical Engineering, College of Engineering, Universiti Teknologi MARA, Shah Alam, Malaysia
[2]Mimos Berhad, Technology Park Malaysia, Kuala Lumpur, Malaysia

Article Info

Article history:

Received Feb 7, 2024
Revised May 24, 2024
Accepted Jun 19, 2024

Keywords:

Extended gate field effect transistor
Internet of things
Long-range wide area network
Potentiometric sensing
Sensor interfaces

ABSTRACT

This research paper explores the application of extended-gate field-effect transistors (EGFET) as a potentiometric sensing method for pH detection within an internet of things (IoT) system. The pH EGFET sensor is integrated with a long-range (LoRa) microcontroller, enabling data transmission via a low-power, long-range wide-area network (LoRaWAN) IoT framework to a dedicated IoT application server. The framework utilizes a message queuing telemetry transport (MQTT) broker, employing a publish/subscribe message architecture for efficient data transmission. The study focuses on addressing the problem of determining whether EGFET technology can provide precise and dependable measurements in various settings. To achieve this, the data from the IoT framework is compared with data signals from a semiconductor parametric analyzer and a readout interfacing circuit serial data acquisition (DAQ). From the study, EGFET sensors provide a sensitivity of 61.1 mV/pH with a linearity of 0.9968 through the IoT method. Meanwhile, non-IoT methods yield slightly different sensitivities of 53.1 and 50.5 mV/pH with comparable linearity of 0.9984 and 0.9979. Overall, the research demonstrates the versatility of EGFET technology, highlighting its effective use in various sensing instruments, while ensuring reliable data transfer through the LoRaWAN framework.

Corresponding Author:

Wan Fazlida Hanim Abdullah
Integrated Sensors Research Group, School of Electrical Engineering, College of Engineering
Universiti Teknologi MARA
40450, Shah Alam, Selangor, Malaysia
Email: wanfaz@uitm.edu.my

1. INTRODUCTION

Sensors are devices that produce a voltage in response to what they measure [1]. Among various sensor types, potentiometric sensors stand out for their ability to detect ions [2]. An extended-gate field-effect transistor (EGFET) is an example of a potentiometric sensor where the gate terminal is externally connected and independent of the transistor [3]. Unlike conventional field-effect transistors (FETs), the EGFET physically separates the sensing membrane (where ions are captured) from the gate area. The sensing membrane generates a surface potential that modulates the channel current between the drain and source terminals of the metal-oxide-semiconductor field-effect transistor (MOSFET).

EGFET sensors face challenges related to the development of suitable sensing layers and the design of readout circuitry [4]. These sensors employ a dip and measure technique, where changes in threshold voltage correspond to ion activity when the sensing layer interacts with the target analyte [5]. In this study, the EGFET sensor was used to measure and analyze pH values by detecting hydrogen ions in a solution. The end goal is to adapt this EGFET pH sensor for soil pH detection in large agricultural areas. Therefore, the EGFET sensor was integrated with the internet of things (IoT) system to allow scalability [6]. While Wi-Fi is commonly used for IoT connectivity, this study explores the potential of long-range wide-area network (LoRaWAN) technology as it offers advantages such as lower power consumption and wider coverage [7], [8].

The LoRaWAN IoT framework has two main parts: the LoRaWAN architecture and the application server. The architecture includes end devices, a gateway, and a network server [9]–[11]. These end devices transmit data messages to the gateway via LoRa radio frequency (RF) modulation, connecting to the things network (TTN) server using an authenticated application programming interface (API) key. The TTN server also processes and validates information from the end devices [12].

The IoT architecture is built around core system applications [13], including the InfluxDB database, Node-RED automation platform, Mosquitto communication protocols, and the Grafana dashboard. Data from the TTN server is collected using the lightweight message queuing telemetry transport (MQTT) protocol [14], [15], which employs a Pub/Sub architecture. Node-RED simplifies system development with color-coded building blocks [16] and passes the data to InfluxDB, which is known for its superior performance in handling time series data [17], [18]. The data will then be sent to Grafana, which offers interactive visualization and additional features for event tracking [19].

The study builds upon existing research, incorporating the sensing membrane recipe by Zulkefle *et al.* [20] and the EGFET readout interfacing circuitry designed by Guliga *et al.* [21]. The current EGFET pH soil sensors do not come with any connectivity chip or any connectivity module to communicate with LoRaWAN and the IoT system. Therefore, the study aims to prepare an EGFET pH sensor with LoRaWAN connectivity for soil sensing, ensuring data storage and visualization within the LoRaWAN IoT framework. The experiments in this study are conducted to demonstrate the consistent performance of the EGFET sensor in terms of sensitivity and linearity, as well as its effective integration with LoRaWAN. The following methodology sections will cover the experimental setup, LoRaWAN server configuration, and proposed cloud applications for IoT integration.

2. RESEARCH METHOD

To prepare for sensor validation, the EGFET sensor was tested with a commercial pH buffer solution from Supelco Inc., and RE-1B (Ag/AgCl) from ALS Co., Ltd which acts as the reference electrode. The buffer solution had concentrations of 2, 4, 7, 10, and 12. Three measurement instruments are used to collect sensor data: a data acquisition (DAQ) instrument from Texas Instruments, the B1500A semiconductor device parameter analyzer (B1500) from key sight technologies, and a LoRa TTGO microcontroller connected to the IoT server. The following subsections will explain the measurement setup for all measurement instruments and the IoT server setup.

2.1. The measurement method setup

To detect the pH ions activity, the sensing layer of an EGFET will be dipped inside the pH buffer, along with a grounded reference electrode which serves as a stable reference point to the gate of the MOSFET as shown in Figure 1. This way, any changes in the behavior of the MOSFET's gate are only due to the influence of the analyte on the sensing layer. For measurement with DAQ, EGFET was paired with the interfacing circuitry connected to the NI DAQ module. The final output voltage was determined as an average of voltages over time using NI DAQExpress software connected via a USB cable. This measurement method requires pairing the sensing layer with a MOSFET in a constant voltage constant current (CVCC) circuitry biasing [22], sharing the same ground as the reference electrode.

Meanwhile, for the B1500 instrument, the source-measure unit (SMU) 1 of the B1500 was linked to the reference electrode, SMU 2 to the MOSFET's drain terminal, and SMU 3 to the source terminal as shown in Figure 2. The MOSFET's gate terminal was connected to the sensing layer where the gate voltage (V_g) was swept from 0 to 3 V, creating a transfer curve of gate voltage against drain current (Id) at a constant drain voltage (Vd) of 100 mV. The output voltage was measured at the isothermal point, where the drain-source current (Ids) remained constant across various temperature differences [23].

The last measurement method with LoRaWAN was also paired with the interfacing circuitry, but this time, the output was connected to the analog-to-digital converter (ADC) input pin of the TTGO LoRa32 microcontroller module as shown in Figure 3. This module features a built-in antenna for detecting LoRa modulation therefore the resulting output voltage readings are transmitted by the LoRa transmitter to the application server via the LoRaWAN gateway. The microcontroller measures analog inputs at a lower sampling rate compared to DAQ specifically 5 samples per second due to code limitations. Each measurement for different pH buffer concentrations is repeated 3 times, with a 30-second delay between each measurement. The output voltage is saved in a comma-separated value (CSV) file and plotted in Microsoft Excel software.

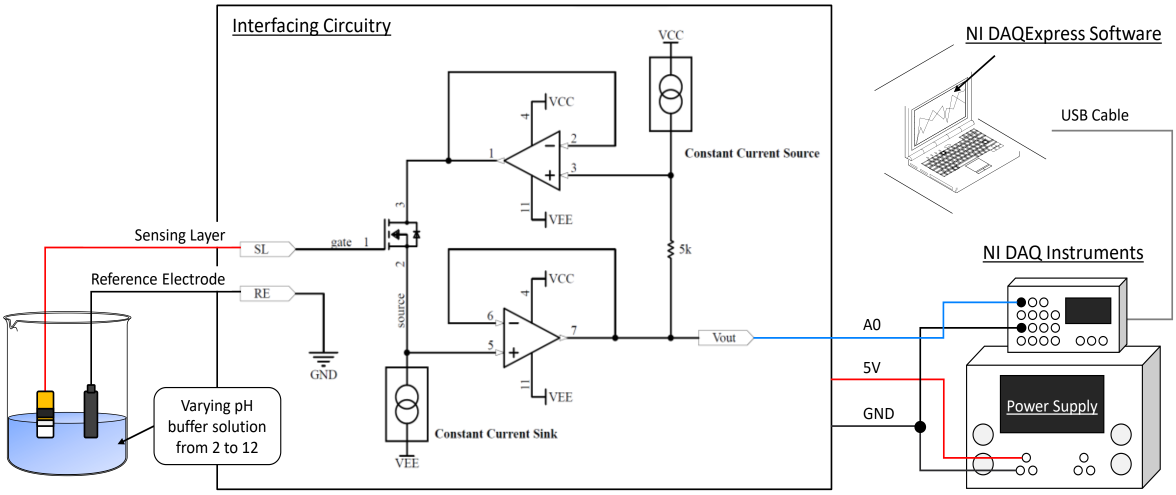

Figure 1. Obtaining averaged data over time with DAQ

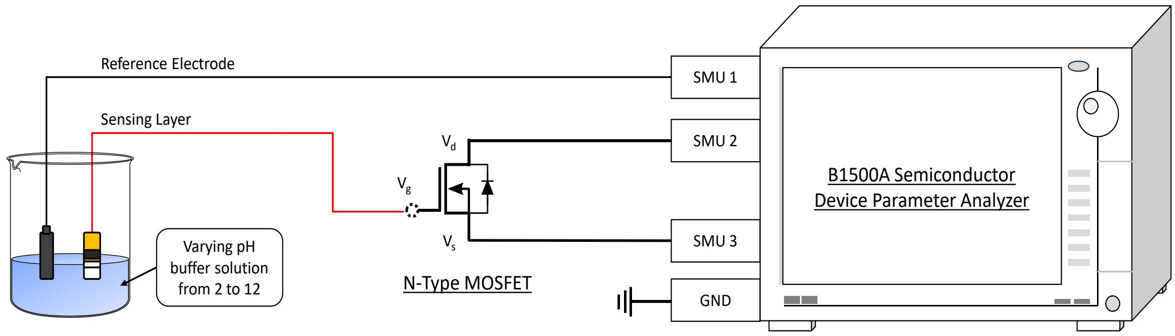

Figure 2. B1500 measurement setup for MOSFET characterization

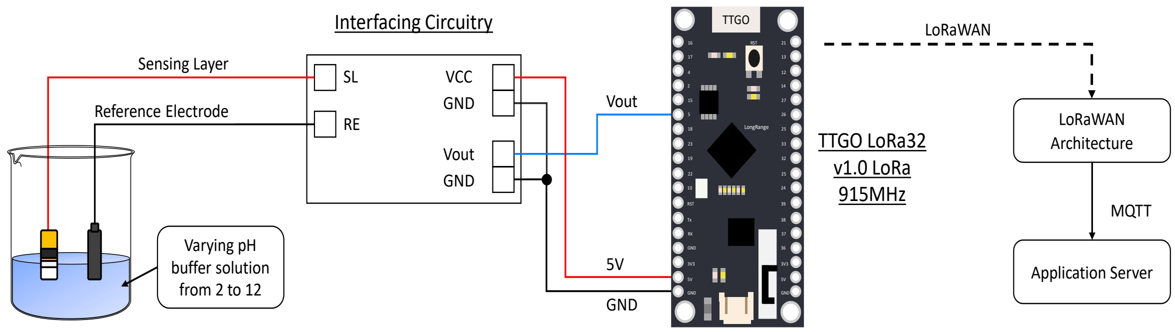

Figure 3. Obtaining averaged data over time with a microcontroller via LoRaWAN

2.2. The LoRaWAN internet of things framework

Figure 4 illustrates the two primary components of the LoRaWAN IoT framework: the LoRaWAN architecture (comprising end nodes, a gateway, and TTN) and the application server (which includes the Node-RED application, InfluxDB database, and Grafana dashboard). This subsection provides details on configuring the LoRaWAN gateway, TTN server, and the application server.

In the Dragino DLOS8 gateway configuration page of Figure 5, the LoRa configuration, LoRaWAN configuration (IoT service), and Wi-Fi access point are configured. Table 1 provides a concise summary of the required changes and the reasons for tailoring the gateway configurations to be used in Malaysia. Both the LoRa microcontroller and the gateway must be added to TTN by registering their end-device identifier. Figure 6 highlights the TTN application interface along with a sample of payload data from the end nodes in JavaScript object notation (JSON) format. The measurement data are organized under the decoded payload messages and all this data is forwarded to the application server.

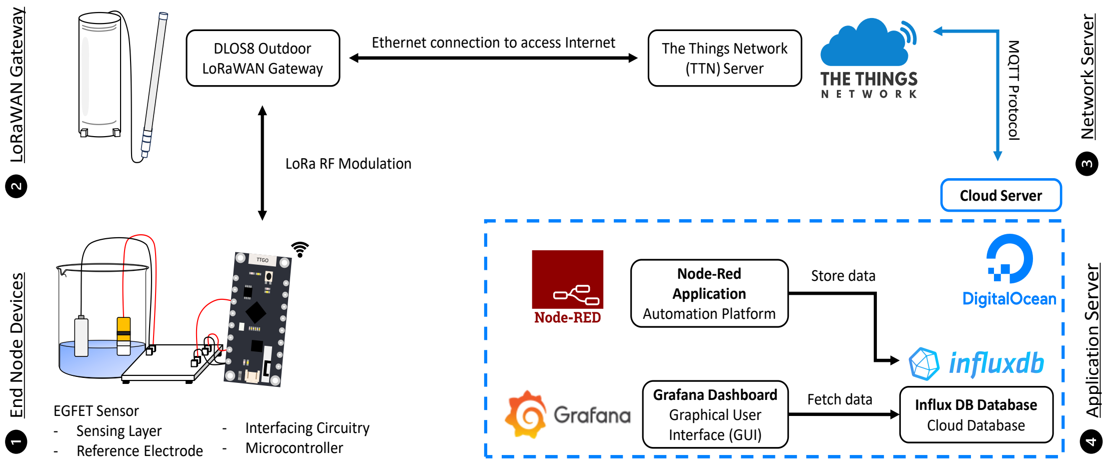

Figure 4. The LoRaWAN IoT framework

Figure 5. DLOS8 Dragino gateway configuration page

Table 1. Summary for changes in Dragino DLOS8 gateway configuration

Parent-category	Sub-category	Value	Remarks
LoRa configuration	Frequency plan	Asia 920 to 923 MHz	Frequency of LoRaWAN in Malaysia
IoT service	Server's address	au1.cloud. the things.network	TTN server for the region
	Uplink port	1700	To match TTN settings
	Downlink port	1700	To match TTN settings
Wi-Fi access point	Wi-Fi access point	Follows the SSID of the gateway	Located at the back of the box upon purchasing the gateway
	Wi-Fi WAN client	Follows the Wi-Fi credentials and password	Referring to the router with Internet connection

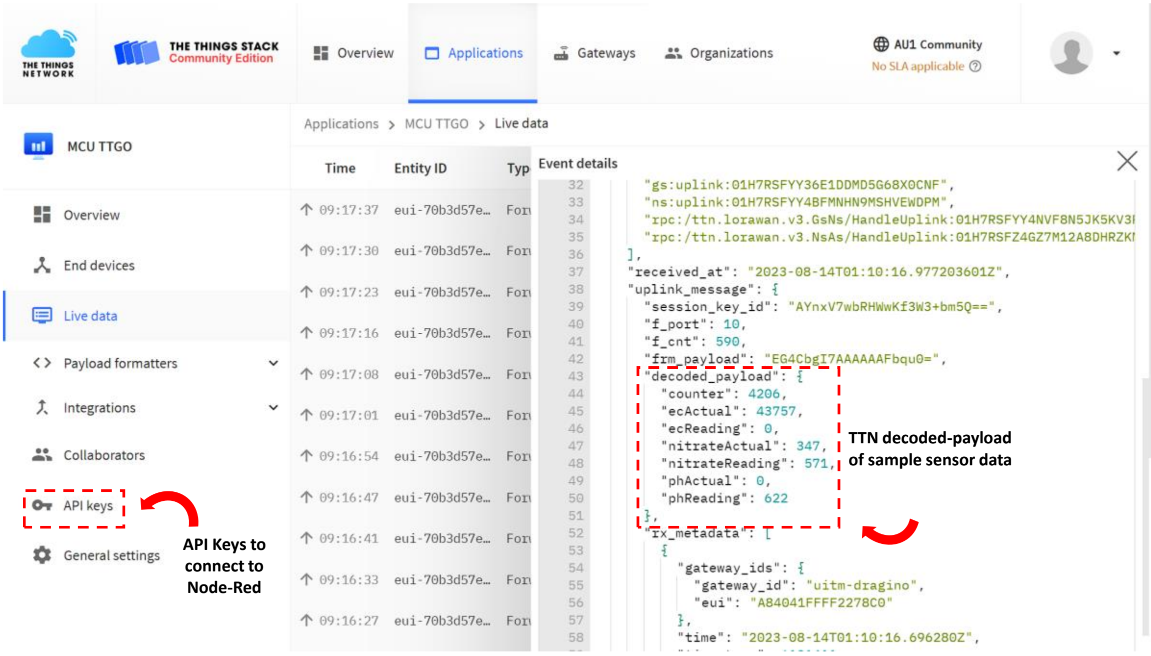

Figure 6. TTN network server application interface

The application server is a cloud server subscribed with Digital Ocean hosted on an Ubuntu version 22.10 operating system equipped with a regular Intel CPU and 25 GB SSD. In Figure 7, the MQTT node in Node-RED receives data from TTN, then filters the required information and formats the data according to the database requirements. This output data saved in InfluxDB is automatically formatted in tables based on elapsed time as shown in Figure 8. Finally, Grafana will retrieve data from the database and present it in charts and line graphs. To integrate the database with Grafana, add it as a data source in the data source tab within Grafana's settings.

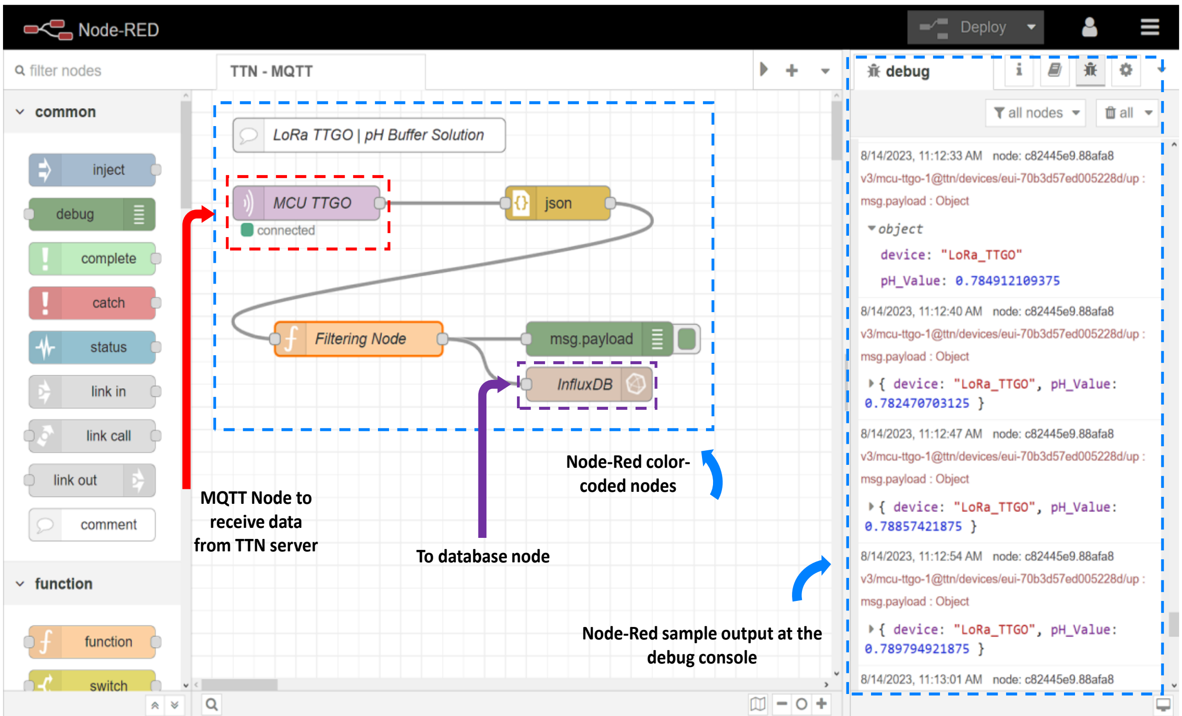

Figure 7. Node-RED blocks and output node

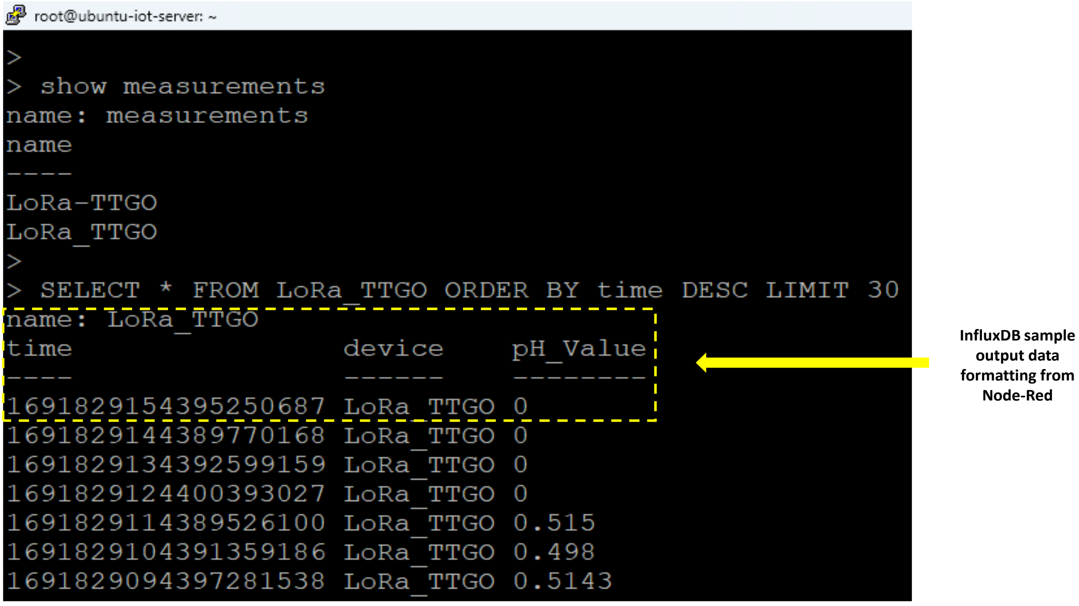

Figure 8. InfluxDB database data structure

3. RESULTS AND DISCUSSION

This chapter presents the results of the study and discusses their implications. This study looks into the sensor behavior with IoT, which the previous studies didn't. Output reading from measurement instruments is shown in Figure 9. Characterizing TiO2 samples using the B1500 analyzer yields the left graph of drain current against gate voltage in Figure 9(a). The sensing layer used in each method differs from each other, but it was fabricated within the same batch. As V_g increases above the threshold voltage (V_{th}) of the MOSFET around 0.7 V, the device begins to conduct more current, resulting in an increase in the slope of the I_d vs. V_g curve. The final output voltage is taken at the isothermal point where the current is 100 uA. Next, Figure 9(b) displays the sensor reading in NI DAQExpress software. The yellow line represents the collected input data over time, and the 'Input 0' that reads an initial voltage of 351 mV or 0.351 V corresponds to the connected DAQ input port to the sensing layer. Lastly, Figure 9(c) shows the graph of sensor data at the Grafana dashboard. These graphs serve as evidence that data are stored in the database, and Node-RED successfully parses data from TTN to InfluxDB.

Table 2 provides a comprehensive summary of results across all measurement methods, focusing on average voltage values, sample sensitivity, and linearity. Meanwhile, the graph in Figure 10 visually represents the data plotted in Table 2. The slope of the graph or the gradient of the linear equation represents the sensitivity of the sensor, while the regression factor (R^2) indicates the linearity of the relationship [24]. According to the figure, the pH sensitivity of the sample in B1500 is found to be 53 mV/pH, with a linearity of 0.9984. This value aligns with the Nernstian behavior of 59 mV/pH [25] which implies that the sensor responds predictably and consistently across a wide pH range. Meanwhile, for the pH sensor in DAQ, an increase in pH value corresponds to a decrease in the averaged output voltage reading. The graph exhibits a negative slope, which diverges from the trend observed using the B1500 instrument with a slightly lower sensitivity of 50.5 mV/pH, but a constant linearity of 0.9979. The difference arises due to variations in how the instruments are designed internally. The B1500 instrument is a parametric analyzer that is swept behavior while the interfacing circuitry is point biasing therefore their behavior to response to changes in pH is different.

Lastly, in the LoRaWAN IoT framework, the pH sensitivity of the sample was determined to be 61.1 mV/pH, with a consistent linearity of 0.9968. The LoRaWAN sample appears slightly more sensitive, possibly due to unforeseen disturbances during the sensing layer deposition process in sample preparation. Regardless, the decreasing voltage trend remains consistent with NI DAQ. When examining each row of the pH values, it becomes evident that the voltages may not be identical. However, the crucial observation lies in the consistent trend of an incremental increase or decrease of approximately 0.05V/pH value. When the voltage adheres to this trend, the sensitivity and linearity align with what is observed using the B1500 and DAQ instruments.

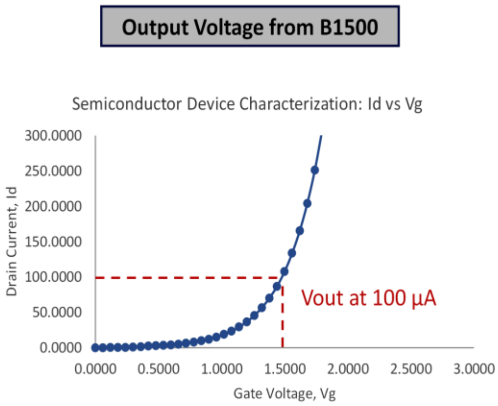

(a)

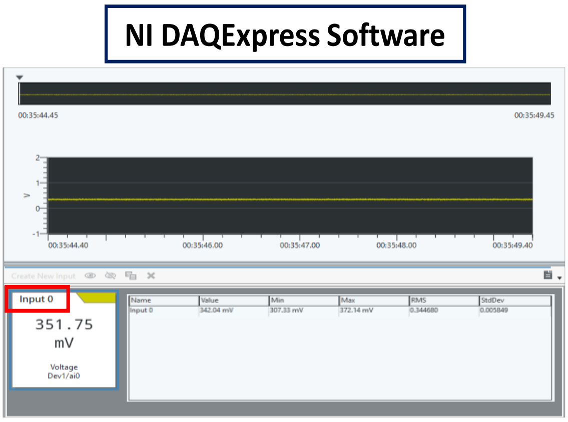

(b)

(c)

Figure 9. Output reading from measurement instruments (a) B1500 analyzer, (b) NI DAQExpress software, and (c) Grafana dashboard

Table 2. Results summary for all measurement methods

Topic	pH value	B1500	DAQ	LoRaWAN
Average voltage values	2	1.1143	1.1103	1.1147
	4	1.0247	1.0130	1.0167
	7	0.8413	0.8517	0.8445
	10	0.6297	0.6500	0.6411
	12	0.4980	0.5150	0.5091
Sensitivity	Not applicable	53.1 mV/pH	50.5 mV/pH	61.1 mV/pH
Linearity	Not applicable	0.9984	0.9979	0.9968

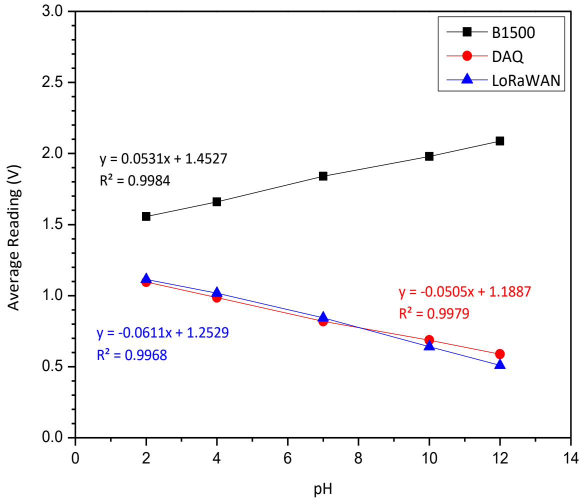

Figure 10. Comparison of voltage response characteristics with 3 different instruments

4. CONCLUSION

In conclusion, the main findings indicate that the pH EGFET sensor consistently maintains sensitivity and linearity across various measurement instruments. The successful IoT server setup allowed pH EGFET sensor data to be transmitted to the TTN server, filtered through Node-Red, stored in InfluxDB, and displayed via Grafana. Integrating the EGFET with LoRaWAN IoT at a low sampling rate does not result in data loss. However, the sensor's sensitivity deviated slightly from the expected Nernstian behavior (61.1 mV/pH), possibly due to unforeseen disturbances during fabrication or insufficient data averaging at the IoT server's output. The consistent behavior of pH EGFET suggests that other EGFET sensors may exhibit similar characteristics, expanding their potential use as IoT sensors in various industries. Additionally, the successful LoRaWAN integration opens possibilities for further testing, such as longer distances or environments with more signal interference. To enhance the research, future work could focus on improving the microcontroller code to send more data to LoRaWAN IoT or implementing averaging techniques for improved accuracy. Additionally, exploring aspects like the actual power consumption, crosstalk between devices, and effective communication distance for LoRaWAN would also be beneficial.

ACKNOWLEDGEMENTS

The research project is funded by the Ministry of Higher Education (MOHE) under the Fundamental Research Grant Scheme (FRGS)(FRGS/1/2022/TK07/UITM/02/38) and supported by the College of Engineering, Universiti Teknologi MARA.

REFERENCES

[1] F. R. Simões and M. G. Xavier, "Electrochemical sensors," in *Nanoscience and its Applications*, Elsevier, 2017, pp. 155–178, doi: 10.1016/B978-0-323-49780-0.00006-5.
[2] B. W. An *et al.*, "Smart sensor systems for wearable electronic devices," *Polymers*, vol. 9, no. 8, p. 303, Jul. 2017, doi: 10.3390/polym9080303.
[3] N. Mokhtarifar, F. Goldschmidtboeing, and P. Woias, "Indium tin oxide coated pet for differential ph-sensing using field-effect transistor based sensor," *Micro & Nano Letters*, vol. 13, no. 11, pp. 1525–1530, Nov. 2018, doi: 10.1049/mnl.2018.5240.
[4] S. Sinha and T. Pal, "A comprehensive review of fet-based ph sensors: materials, fabrication technologies, and modeling," *Electrochemical Science Advances*, vol. 2, no. 5, Oct. 2022, doi: 10.1002/elsa.202100147.
[5] P. Sharma *et al.*, "Hydrogen ion sensing characteristics of na3bio4–bi2o3 mixed oxide nanostructures based Egfet ph sensor," *International Journal of Hydrogen Energy*, vol. 45, no. 37, pp. 18743–18751, Jul. 2020, doi: 10.1016/j.ijhydene.2019.07.252.
[6] Y. Xu and A. Helal, "Scalable cloud–sensor architecture for the internet of things," *IEEE Internet of Things Journal*, vol. 3, no. 3, pp. 285–298, Jun. 2016, doi: 10.1109/JIOT.2015.2455555.
[7] P. Ferreira, R. N. Miranda, P. M. Cruz, and H. S. Mendonca, "Multi-protocol lorawan/WI-FI sensor node performance assessment for industry 4.0 energy monitoring," in *2019 IEEE-APS Topical Conference on Antennas and Propagation in Wireless Communications (APWC)*, IEEE, Sep. 2019, pp. 403–407, doi: 10.1109/APWC.2019.8870468.
[8] G. Klimiashvili, C. Tapparello, and W. Heinzelman, "LoRa vs. WIFI ad HOC: a performance analysis and comparison," in *2020 International Conference on Computing, Networking and Communications (ICNC)*, IEEE, Feb. 2020, pp. 654–660, doi: 10.1109/ICNC47757.2020.9049724.
[9] A. Tayebi, L. Veltri, F. Zanichelli, and S. Caselli, "Interworking between lorawan and non-lora IoT systems," in *2022 IEEE International Conference on Pervasive Computing and Communications Workshops and other Affiliated Events (PerCom*

Workshops), IEEE, Mar. 2022, pp. 415–420, doi: 10.1109/PerComWorkshops53856.2022.9767494.
[10] D. Singh *et al.*, "LoRaWAN gateway architecture for aquaculture monitoring in rural area," *2023 6th International Conference on Information Systems and Computer Networks, ISCON 2023*, 2023, doi: 10.1109/ISCON57294.2023.10111936.
[11] G. Codeluppi, A. Cilfone, L. Davoli, and G. Ferrari, "LoRaFarM: a lorawan-based smart farming modular IoT architecture," *Sensors*, vol. 20, no. 7, p. 2028, Apr. 2020, doi: 10.3390/s20072028.
[12] O. T. Sanchez, D. Raposo, A. Rodrigues, F. Boavida, and J. Sá Silva, "Private lorawan network gateways: assessment and monitoring in the context of iIoT-based management," in *XXXI Conference on Electrical and Electronic Engineering*, Basel Switzerland: MDPI, Dec. 2023, p. 4, doi: 10.3390/engproc2023047004.
[13] S. Wang and H. Yan, "Design of real-time monitoring platform for internet of things based on cloud platform," in *2020 IEEE 5th Information Technology and Mechatronics Engineering Conference (ITOEC)*, IEEE, Jun. 2020, pp. 61–64, doi: 10.1109/ITOEC49072.2020.9141881.
[14] G. C. Hillar, "MQTT essentials - a lightweight IoT protocol," *Journal of Chemical Information and Modeling*, vol. 53, no. 9, p. 273, 2017.
[15] M. Cimdins, F. John, and H. Hellbrück, "Flexible data acquisition with lorawan and MQTT for small and medium-sized enterprises," *Mobilkommunikation: Technologien und Anwendungen - 25. ITG-Fachtagung*, pp. 87–92, 2021.
[16] A. N. Rosli, R. Mohamad, Y. W. M. Yusof, S. Shahbudin, and F. Y. A. Rahman, "Implementation of mqtt and lorawan system for real-time environmental monitoring application," in *2020 IEEE 10th Symposium on Computer Applications & Industrial Electronics (ISCAIE)*, IEEE, Apr. 2020, pp. 287–291, doi: 10.1109/ISCAIE47305.2020.9108808.
[17] M. Ali, A. Alqahtani, M. W. Jones, and X. Xie, "Clustering and classification for time series data in visual analytics: a survey," *IEEE Access*, vol. 7, pp. 181314–181338, 2019, doi: 10.1109/ACCESS.2019.2958551.
[18] S. Di Martino, L. Fiadone, A. Peron, A. Riccabone, and V. N. Vitale, "Industrial internet of things: persistence for time series with NOSQL databases," in *2019 IEEE 28th International Conference on Enabling Technologies: Infrastructure for Collaborative Enterprises (WETICE)*, IEEE, Jun. 2019, pp. 340–345, doi: 10.1109/WETICE.2019.00076.
[19] Y. A. Ahmad, T. S. Gunawan, M. H. M. R. Al Munir, N. M. Yusoff, M. Kartiwi, and H. Mansor, "Development of visual dashboard for river monitoring system," in *2022 IEEE 8th International Conference on Smart Instrumentation, Measurement and Applications (ICSIMA)*, IEEE, Sep. 2022, pp. 267–272, doi: 10.1109/ICSIMA55652.2022.9928973.
[20] M. A. Zulkefle *et al.*, "EVALUATION on the egfet ph sensing performance of sol-gel spin coated titanium dioxide thin film," *Jurnal Teknologi*, vol. 83, no. 4, pp. 119–125, Jun. 2021, doi: 10.11113/jurnalteknologi.v83.16313.
[21] H. Guliga, W. F. H. Abdullah, and S. H. Herman, "Extended gate field effect transistor (EGFET) integrated readout interfacing circuit for ph sensing," in *2014 2nd International Conference on Electrical, Electronics and System Engineering (ICEESE)*, IEEE, Dec. 2014, pp. 11–14, doi: 10.1109/ICEESE.2014.7154605.
[22] W. F. H. Abdullah, M. Othman, and M. A. M. Ali, "Chemical field-effect transistor with constant-voltage constant-current drain-source readout circuit," in *2009 IEEE Student Conference on Research and Development (SCOReD)*, IEEE, 2009, pp. 219–221, doi: 10.1109/SCORED.2009.5443112.
[23] N. I. M. Noh, K. A. Yusof, M. Zolkapli, A. Z. Abdullah, W. F. H. Abdullah, and S. H. Herman, "Effect of channel width-to-length ratio on isothermal point of mosfet-isfet structure," in *RSM 2013 IEEE Regional Symposium on Micro and Nanoelectronics*, IEEE, Sep. 2013, pp. 130–133, doi: 10.1109/RSM.2013.6706490.
[24] B. Skiera, J. Reiner, and S. Albers, "Regression analysis," in *Handbook of Market Research*, vol. 382, no. 8520, Cham: Springer International Publishing, 2018, pp. 1–29, doi: 10.1007/978-3-319-05542-8_17-1.
[25] M. Hussain, Z. H. Ibupoto, M. A. Abbasi, O. Nur, and M. Willander, "Effect of anions on the morphology of CO_3O_4 nanostructures grown by hydrothermal method and their pH sensing application," *Journal of Electroanalytical Chemistry*, vol. 717–718, pp. 78–82, Mar. 2014, doi: 10.1016/j.jelechem.2014.01.011.

BIOGRAPHIES OF AUTHORS

Akmal Mustaffa Zulhakim is a Master of Science student at Universiti Teknologi MARA. He received his Bachelor of Engineering (Hons.) Electronics Engineering from Universiti Teknologi MARA, Malaysia, in 2022. His research interests include sensor interfacing circuitry, circuit design, computer programming, the Internet of Things, and cloud server configurations, and his recent projects are related to those areas. He can be contacted at email: 2022494002@student.uitm.edu.my or akmalmustaffa99@gmail.com.

Wan Fazlida Hanim Abdullah is an Assistant Professor at the School of Electrical Engineering, College of Engineering, Universiti Teknologi MARA, Malaysia. Her research interests include microelectronic devices, solid-state sensors, nanoelectronics, and sensor-interfacing circuits. Her recent projects are extended-gate field-effect transistor sensing development and sensor system solutions for applications supporting Sustainable Development Goals. She can be contacted at email: wanfaz@uitm.edu.my.

Ahmad Zaki Abu Bakar is currently a Senior Staff Engineer at the Wireless Innovation laboratory in MIMOS. His primary role is to realize intercommunication between various hardware devices in terms of embedded software programming. He is also responsible for designing and implementing the device's end-to-end software flow for the integration with MIMOS IOT platform. He has vast working experience with various roles and responsibilities within the embedded system development in multinational and local companies. He holds a Bachelor's Degree in Electrical and Electronics Engineering from Salford University, United Kingdom. Ahmad Zaki holds 11 patents (2 granted, 9 filed). He can be contacted at email: zaki.bakar@mimos.my.

Robaiah Mamat completed her Ph.D. in Graphene Nanomaterial at the Faculty of Applied Sciences, Universiti Teknologi MARA. She received her MSc. In Superconductor Material at the Faculty of Applied Sciences, Universiti Teknologi MARA. She graduated with honors in Bac. Sc. (Hons) Physics from the Universiti Teknologi Mara Shah Alam, Malaysia. She is a research official for Research Grant PRGS, School of Electrical Engineering, College of Engineering, Universiti Teknologi MARA, Malaysia. Her research interests include graphene, nanomaterials, nanoelectronics, and sensor-interfacing circuits. Her recent projects are extended-gate field-effect transistor sensors, which are the development of pH sensors and nitrate sensors with data analytics. She can be contacted at email: robaiahhajimamat@gmail.com or Robaiah_hjmamat@yahoo.com.

Ili Shairah Abdul Halim is a Senior Lecturer in College of Engineering, Univertsiti Teknologi MARA. She received her Bachelor's Degree in Electrical Engineering (Hons) from Universiti Teknologi MARA, Malaysia, in 2007. She obtained her Master of Engineering Science from the University of New South Wales, Australia, in 2009. She currently received her Ph.D. in 2021 from UTM in the area of embedded systems and reconfigurable computing. She can be contacted at email: shairah@uitm.edu.my.

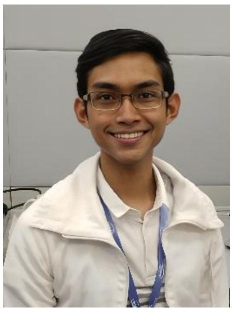

Muhammad Izzat Alif Muslan is a Master of Science student at Universiti Teknologi MARA as well as a Product Development Engineer at Intel Corporation. He obtained his Bachelor of Engineering (Hons.) Electronic Engineering in 2019 from Universiti Teknologi MARA (UiTM) Shah Alam, Selangor, Malaysia. His work involves circuits and systems made for monitoring, particularly in agriculture. He can be contacted at email: 2021722879@student.uitm.edu.my or izzat.alif@hotmail.com.

Sukreen Hana Herman received her Ph.D. (Materials Science) in 2009 from the Japan Advanced Institute of Science and Technology (JAIST). Sukreen was with Sharp-Roxy before pursuing her Master's. She joined Universiti Teknologi MARA (UiTM) in 2004 and now is a senior lecturer at the School of Electrical Engineering, College of Engineering UiTM. She is a member of the Integrated Sensor Research group at the College of Engineering. Her research interests include Fabrication and Characterization of Semiconductor Materials in general and mainly focused on Sensor Applications. She can be contacted at email: hana1617@uitm.edu.my.